

TRANSITION CROSSING IMPROVEMENTS

M. Church

25 April 1991

I. Motivation

During the accelerator studies period of 12/90 - 1/91 efforts were made to improve the efficiency of crossing transition in the Accumulator. E760 wishes to measure the product of the branching ratios for

$$\bar{p}p \longrightarrow \eta_c \longrightarrow \gamma\gamma \quad (1)$$

and the mass and width of the η_c . Since resonance production of the η_c requires a beam momentum of 3.67 GeV/c which is below the Accumulator design transition momentum, and since the above process is rare, it is required to cross transition efficiently (> 90%) with 30 mA of beam. In the past, transition crossing efficiency has been intensity-dependent, with never more than 10 mA getting through transition. At 8 mA or less, transition crossing efficiency was typically 100%. The beam loss is due to a large longitudinal beam blow-up which has been observed many times during transition crossing (see Fig. 1).

II. Transition Crossing Procedure

Beam is decelerated to a momentum of 5.2 GeV/c by slowly ramping down all Accumulator magnets and RF (H=2). Starting at approximately 6.5 GeV/c the quadrupole strengths are ramped so as to distort the Accumulator lattice so that γ_T drops to 5.0. At 5.2 GeV/c the beam is debunched and the quadrupoles alone are ramped so that γ_T rises to 6.2. This is traditionally called a " γ_T jump." The beam is then rebunched and decelerated as before to lower momenta. The quadrupole strengths are ramped such that the design lattice is restored and γ_T is restored to 5.5. Fig. 2 shows γ_T as a function of beam momentum. Beam is stochastically cooled in all 3 dimensions after transition crossing but not before (during normal operation). Just before transition crossing $\eta = -.0075$, and just after transition crossing $\eta = .0058$. The transition crossing part of the ramp consists of 26 separate current steps with 1/2 second pauses between; although the actual transition crossing occurs at a single step—step 15. The changes in the bus currents are as follows:

A:QT	147.3 amps to 125.6 amps	-15.9%
A:LQ	692.5 amps to 758.1 amps	+9.0%
A:QD	137.7 amps to 141.5 amps	+2.7%

A:QF 137.5 amps to 139.5 amps +1.4%

During transition crossing the tunes are kept constant at $Q_h = .615 \pm .002$ and $Q_v = .612 \pm .002$. γ_T , which depends mostly on LQ, is changed approximately linearly with time (see Fig. 3). Since the beam is not centered in the quadrupoles, it is mis-steered by the quadrupoles and the apertures are reduced substantially during transition crossing:

horizontal: 10.2π mm-mrad before transition, 7.0π mm-mrad after transition

vertical: 10.1π mm-mrad before transition, 6.3π mm-mrad after transition.

However, transverse emittances remain adequately small during transition crossing so as not to cause beam loss.

III. Studies

A Monte Carlo simulation¹ of transition crossing indicated that the longitudinal beam blow-up was relatively slow ($\sim 1/2$ sec), and that it was primarily caused by self-bunching of the beam via the longitudinal impedance ($\sim 50k\Omega$) of the ARF1 cavities. The frequency spectrum from the resistive wall monitor (a broadband pickup) had always shown a strong coherent peak at 53 Mhz, which is the resonant frequency of the ARF1 cavities.

For these reasons it was decided to implement the following changes:

- 1) cross transition more quickly;
- 2) short the ARF1 cavities during transition crossing so their shunt impedance is reduced to ~ 0 ;
- 3) short the ARF3 cavity during transition crossing, increasing its resonant frequency to 14 Mhz ($Z \rightarrow \sim 100\Omega$).

Crossing transition more quickly required that steps 12-18 in the quadrupole current ramps be decreased from $1/2$ sec to $1/12$ sec each. Since the response time of the QT power supply is slow, at these setting rates the actual bus current does not immediately correspond to the current setting. Therefore the correct current ramp for this device had to be determined empirically by trial and error. For the other devices, the time scale could simply be reduced by a factor of 6 for the relevant steps. Fig. 4 shows the QT and QDF bus currents as a function of time for the slow ramp ($1/2$ sec per step) and the fast ramp ($1/12$ sec per step for steps 12-18).

The ARF1 short consists of a metal cylindrical sleeve which is motor-driven across the RF gap. The ARF3 short is simply a closed switch across the gap.

Tests with 7 mA of forward protons showed that, by itself, shorting ARF1 eliminated the coherent spike at 53 Mhz during transition crossing, as did the faster ramp by itself. Fig. 5 shows the effect of both the faster ramp and shorting ARF1. The momentum blow-up was also reduced by these modifications. Shorting ARF3, in addition, seemed to make no difference, however the region around 1.2 Mhz was not studied carefully. Transition crossing was later tried with 7 mA of \bar{p} . Fig. 6 shows the longitudinal Schottky spectrum before and after transition crossing. The ratio

$$\Delta p_{below} / \Delta p_{above} = (\Delta f_{below} \eta_{above}) / (\Delta f_{above} \eta_{below}) = .8 \quad (2)$$

¹Q. Wang, thesis to be submitted shortly

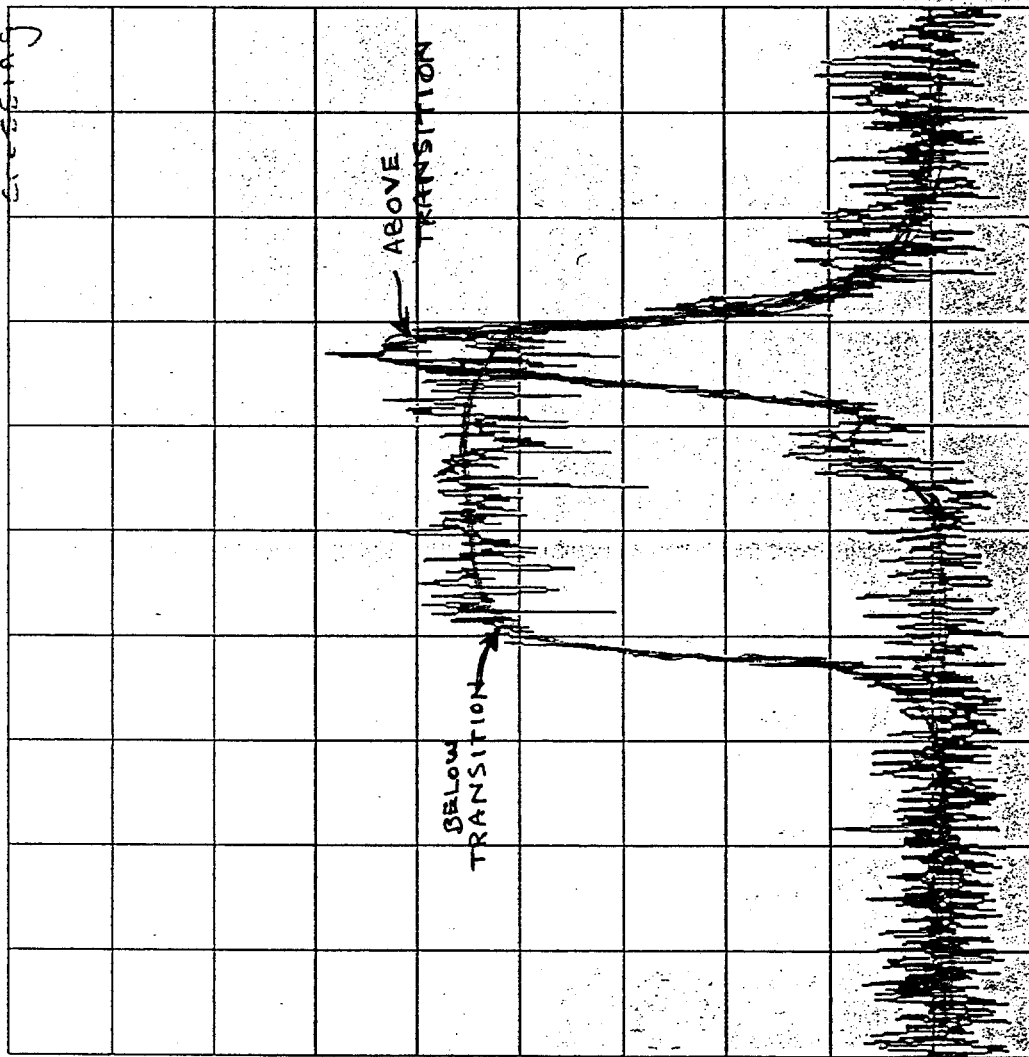
indicates there is no momentum blow-up while crossing transition. Transition crossing was not attempted with 30 mA of forward protons because of possible radiation damage to the E760 Pb-G calorimeter.

IV. Conclusions

For small beam currents (≤ 7 mA) the two modifications—shorting ARF1 and crossing transition more rapidly—eliminate the longitudinal beam blow-up, and the coherent self-bunching of the beam during transition crossing. It is not clear if shorting ARF3 contributes. It remains to be seen if these techniques are effective at 30 mA beam current. All 3 modifications have been integrated into the standard E760 deceleration procedures.

CONSOLE LOCATION 05, MCRL1b 3-JUL-1990 11:01 7 MA \bar{P}
 blow-up at transition cooled before transition crossing

Ref Lvl -30 dB 07/03/90 0915
 Scale 10 dB/div Atten 0 dB Swp 3 500
 Vid BH 100 Hz Res BH 100 Hz



Start Freq 79.03500001 MHz Stop Freq 79.04500001 MHz
 10 kHz span

FIG. 1: Longitudinal Schottky spectrum before and after transition crossing (before transition crossing improvements)

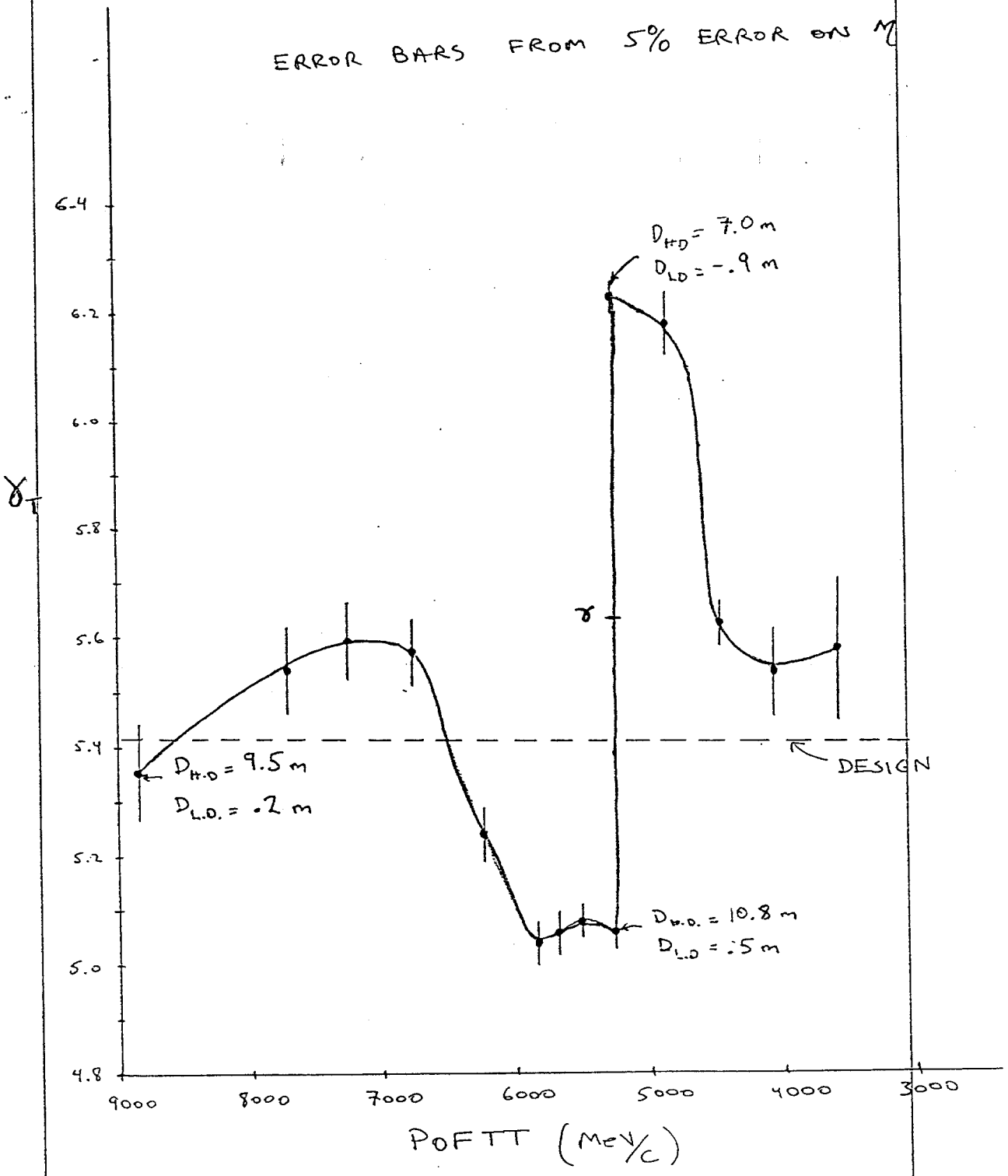


FIG. 2: Transition gamma as a function of beam energy; also shown are the dispersions at the straight sections.

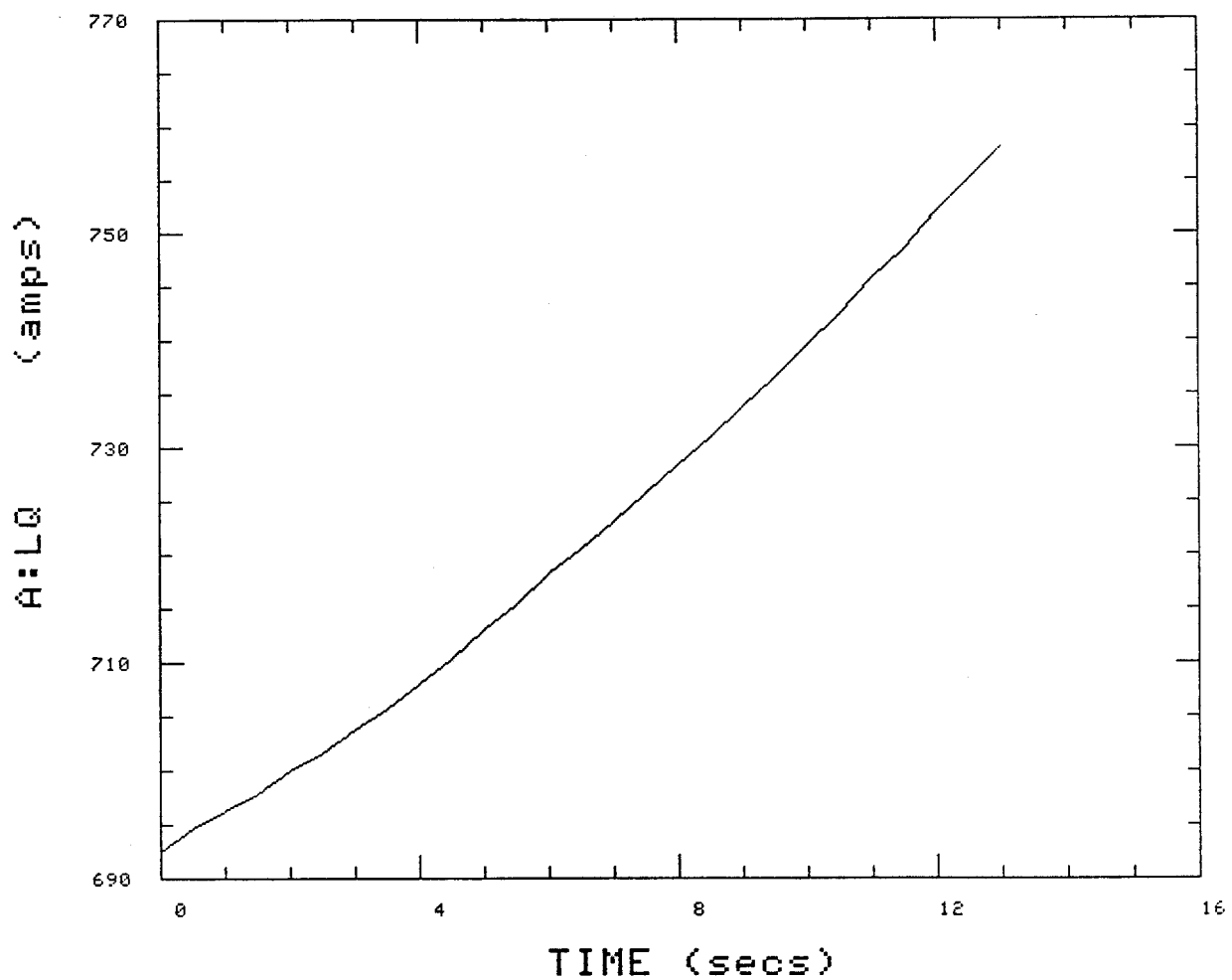
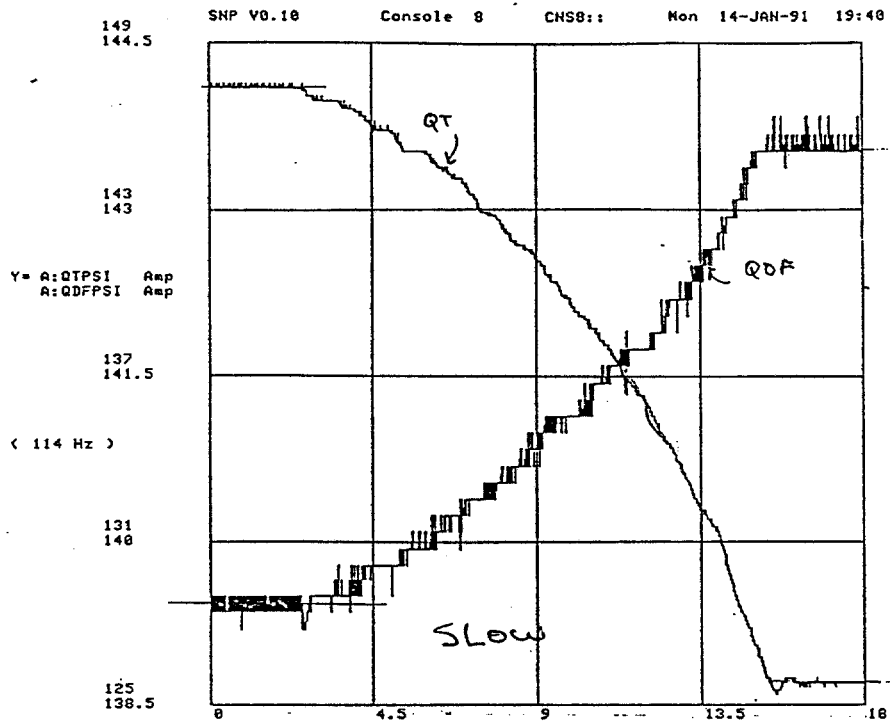
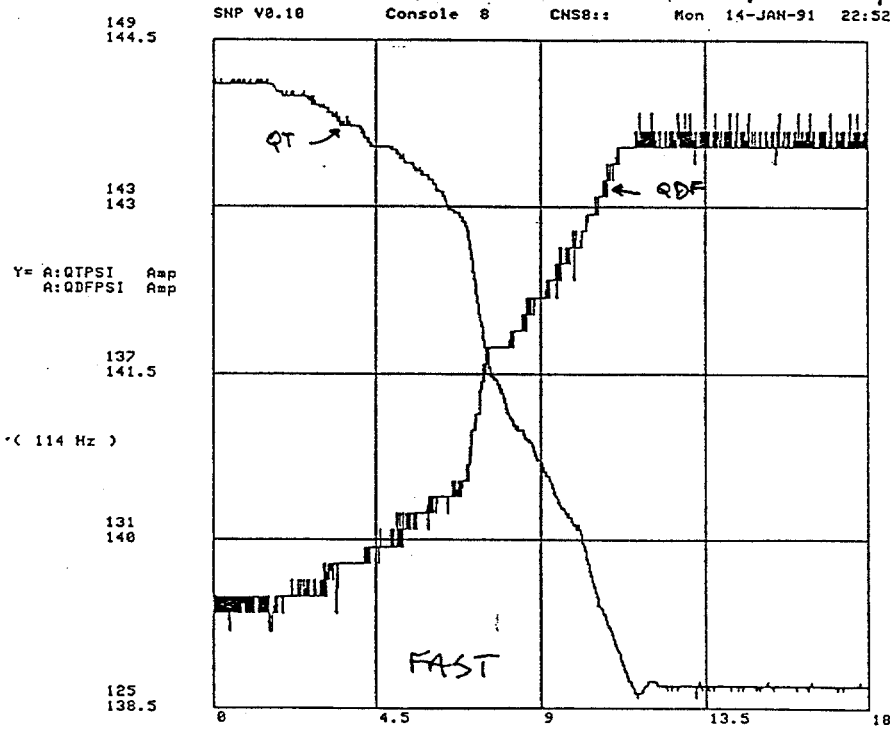


FIG. 3: LQ current settings as a function of time during transition crossing ramp

26 STEPS @ 1/2 SEC/STEP



VIEW Seconds Trig = EVENT OF engineering units
MIDDLE 7 STEPS @ 1/2 SEC/STEP

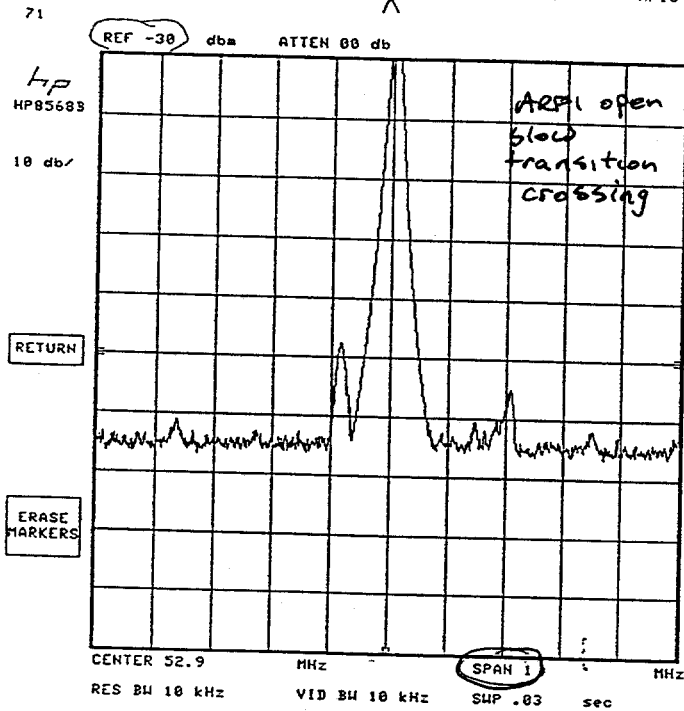


VIEW Seconds Trig = EVENT OF engineering units

FIG. 4: Top plot shows QT and QDF current readback as a function of time during transition crossing for the slow ramp (1/2 sec per step); Bottom plot shows same but for fast ramp (steps 12-18 6 times faster)

RESISTIVE WALL MONITOR

RW MONITOR AT 52.9MHZ, AFTER ET, ARF1 ^{NOT} SHORTED. (MAX HOLD) AP10 RIGH



FORWARD PROTONS

RW MONITOR, AFTER FASTER ET CROSSING, 5.5MA, ARF1 SHORTED. AP10 RI

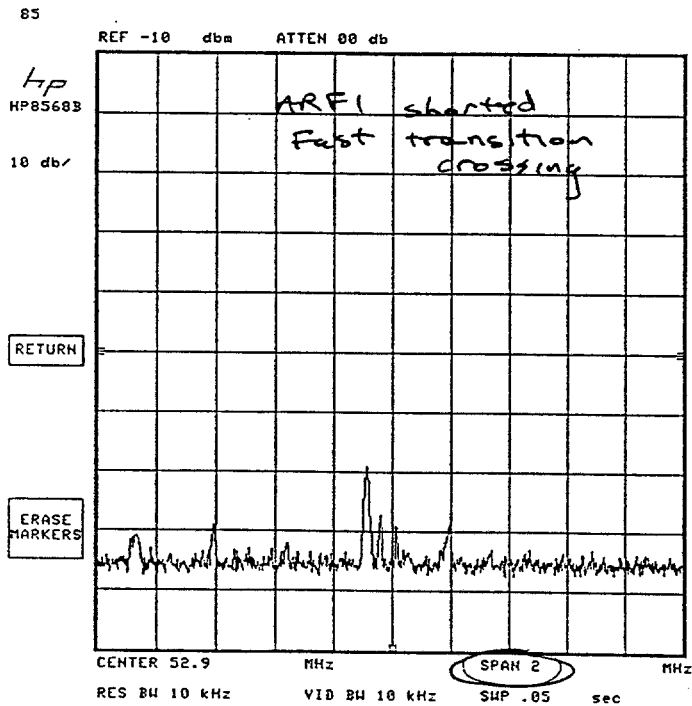


FIG. 5: "Maximum hold" frequency spectrum from resistive wall monitor during transition crossing; top plot is with no improvements and bottom plot is with ARF1 shorted and faster ramp

LONGITUDINAL SCHOTTKY, ~~the~~
 before and after transition, both gaps shorted, fast ramp
 7mA $\bar{0}$
 01/09/91 1607

Scale 10 dB/div
 Atten 10 dB
 Swp 10 sec
 Vid BW 30 Hz
 Res BW 30 Hz

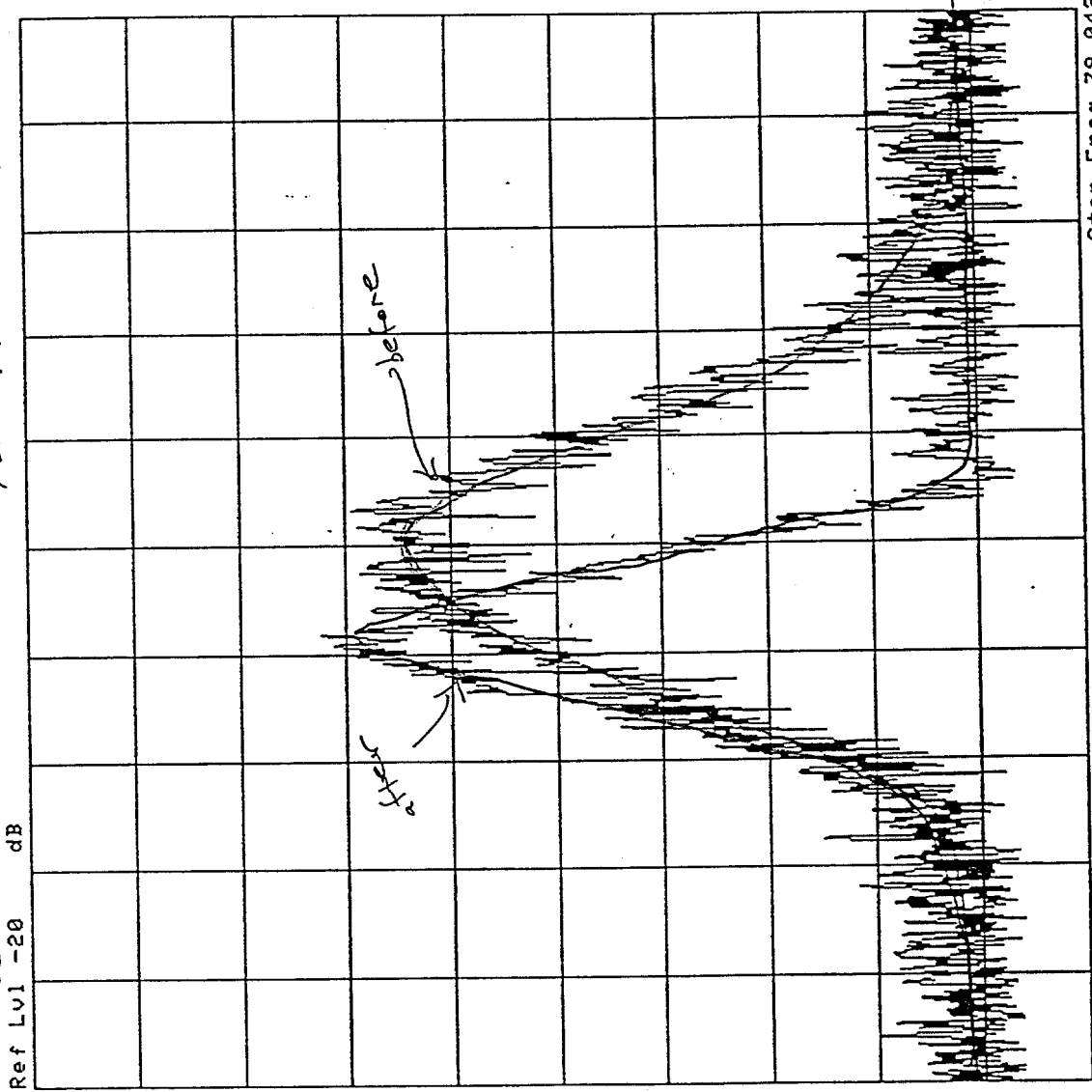


FIG. 6: Longitudinal Schottky spectrum before and after transition (with transition crossing improvements); compare with FIG. 1